

Superconducting RF for energy-recovery linacs

M. Liepe*, J. Knobloch

LEPP, Cornell University, Ithaca, NY 14853, USA
BESSY GmbH, D-12489 Berlin, Germany

Available online 21 November 2005

Abstract

Since superconducting RF for particle accelerators made its first appearance in the 1970s, it has found highly successful application in a variety of machines. Recent progress in this technology has made so-called Energy-Recovery Linacs (ERLs)—originally proposed in 1965—feasible, and interest in this type of machine has increased enormously. A superconducting linac is the driving heart of ERLs, and emittance preservation and cost efficiency is of utmost importance. The resulting challenges for the superconducting cavity technology and RF field control are manifold. In March 2005 the first international workshop on ERLs was held at Newport News, VA, to explore the potential of ERLs and to discuss machine-physics and technology challenges and their solutions. This paper reviews the state-of-the-art in superconducting RF and RF control for ERLs, and summarizes the discussions of the SRF working group on this technology during the ERL2005 workshop.

© 2005 Elsevier B.V. All rights reserved.

PACS: 74.01A; 41.70

Keywords: Radio frequency; Superconductivity; Energy-recovery linacs; Cryo modules

1. Introduction

Superconducting radio frequency (RF) is a mature technology. It has found application in a variety of particle accelerators for quite different physics applications, ranging from nuclear and particle physics to powerful light sources. In many cases, superconducting RF (SRF) technology has actually enabled these machines to become feasible at all, or has resulted in a significant performance boost.

One of the newly evolving applications for SRF are Energy-Recovery Linacs (ERLs). Although some ERLs have been in operation for several years, only recent progress in SRF and accelerator technology has made the full potential of this type of particle accelerator accessible. This has enormously increased the interest in ERLs, and envisioned ERL applications include accelerators for the production of synchrotron radiation, free electron lasers,

high-energy electron cooling devices, and electron–ion colliders.

One of the major components of an ERL are the SRF sections in the injector and the main linac, providing an energy gain of up to a few GeV. The parameter space for the main linac RF is given in Table 1, showing that ERLs are pushing the envelope in many respects. Major challenges for the superconducting (s.c.) cavity modules include among others emittance preservation of a high current beam, strong Higher-Order-Mode (HOM) damping, CW cavity operation with high cryogenic losses, and high required field stability. In addition, efficient linac operation is essential for large scale ERLs. In this paper various aspects of SRF technology are discussed, focusing on ERL applications.

2. Superconducting modules for ERLs

Superconducting modules specifically designed from scratch for ERL applications have not been built so far. However, numerous modules, some operating CW, have been developed for other applications. In many cases these

*Corresponding author. Tel.: +1 607 2554951.

E-mail address: mul2@cornell.edu (M. Liepe).

URL: <http://www.lns.cornell.edu/~liepe/matthias.html>.

may serve as a useful starting point for ERL-module development, the required modifications being dependent on the specific application.

Among the issues that must be addressed are:

- CW operation resulting in fairly high dynamic heat loads.
- High-current operation and the resultant large HOM power that must be extracted to limit the cryogenic load and to ensure stable beam conditions.

Table 1
Typical main linac parameters of existing and planned ERLs

Parameter	Min value	Max value
Linac energy (GeV)	0.02	10
Average current (mA)	10	1000
Bunch charge (nC)	0.01	20
Bunch length (ps)	2	100
Cavity frequency (GHz)	0.7	1.5
Cells per cavity	5	9
Acc. gradient (MV/m)	12	20
Unloaded Q_0	8×10^9	2×10^{10}
Loaded Q_1	2×10^7	1×10^8
HOM power per cavity (W)	10 W	>1000
HOM spectrum, 95% upper frequency (GHz)	1	> 50
Ave./peak RF power per cavity (kW)	0.5/1	25/50
Rms amplitude/phase stability	$10^{-3}/0.1^\circ$	$10^{-4}/0.02^\circ$

- Small bandwidth operation (little net beam loading), which makes the cavity operation particularly susceptible to microphonic detuning.

Currently existing superconducting modules, or modules that are presently under construction include:

- CEBAF style modules developed by TJNAF.
- The 100 mA injector cryomodule presently under construction for the TJNAF FEL.
- The electron-cooler module developed by Brookhaven National Laboratory.
- ELBE module developed by FZ Rossendorf.
- The TTF module developed by the TESLA Collaboration.
- The 100 mA injector cryomodule presently under construction for the Cornell ERL.

These modules are depicted in Fig. 1, with the main parameters being given in Table 2.

3. Cavity designs for ERLs

The cavity design for ERLs is driven by two considerations. First, ERLs accelerate, almost by definition, high currents with designs planned all the way up to 1 A. Thus, efficiently extracting HOMs is essential to avoid beam instabilities and excessive cryogenic loading. Secondly,

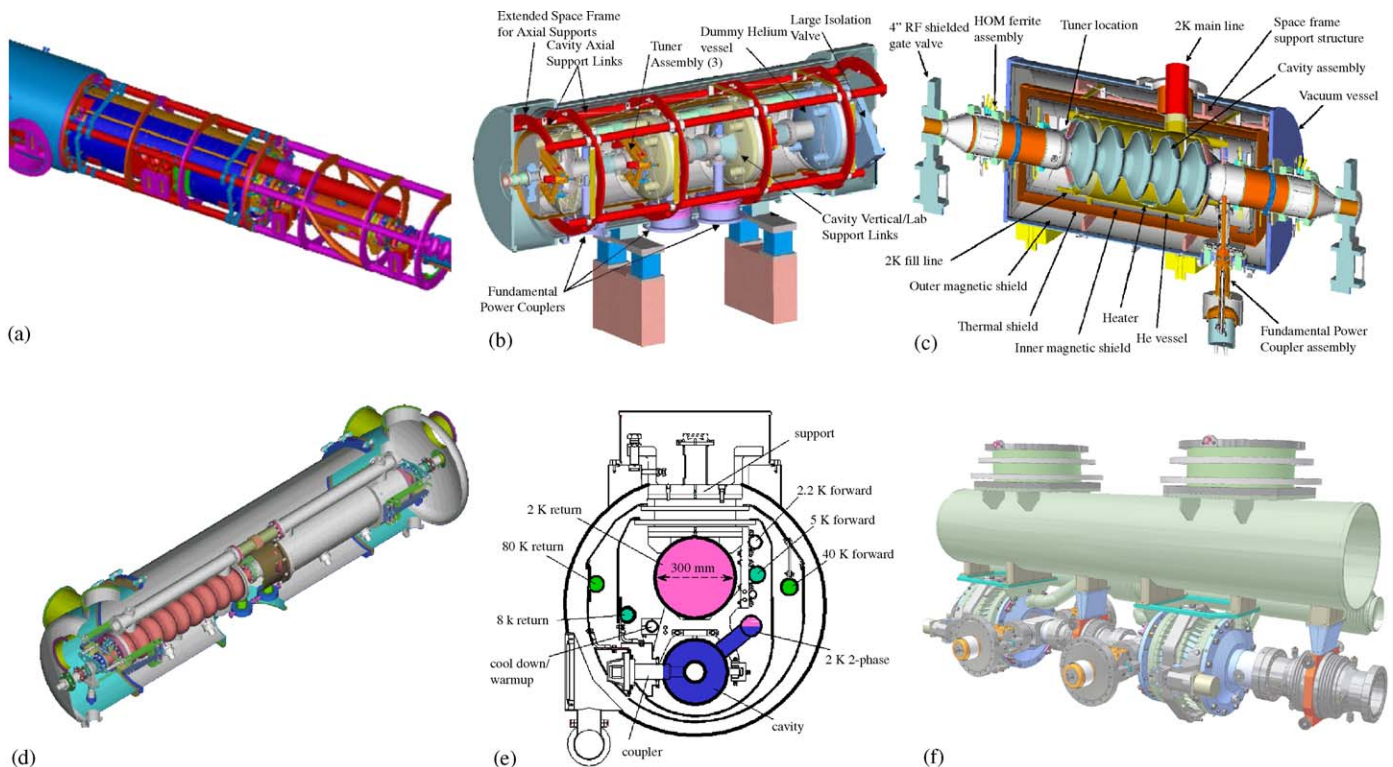


Fig. 1. Examples of SRF cryomodules (existing or under construction). (a) CEBAF upgrade module. (b) TJNAF 100 mA ERL injector. (c) BNL ERL prototype. (d) Rossendorf ELBE FEL. (e) DESY VUV FEL / XFEL. (f) Cornell ERL injector.

Table 2
Examples of SRF cryomodules (existing or under construction)

Parameter	CEBAF upgrade	TJNAF 100 mA ERL injector	BNL ERL prototype
No. of cavities	8	3 + 3rd harmonic	1
Frequency (GHz)	1.5	0.75	0.704
Cells	7	1	5
HOM damping	Loop coupler	Loop coupler	Beam pipe absorber
Duty factor	CW	CW	CW
Temperature (K)	2.1	2.1	2.0
E_{acc} (MV/m)	19 (design)	12.5 (design)	13 (design)
Dynamic heat load (W)	<240	27 (design)	44 (design)
Input coupling	Waveguide	Coaxial	Coaxial
Loaded Q	$<2 \times 10^7$	3×10^5	3×10^7
Peak RF power per cav. (kW)	≈ 10	265	50
CW RF power per cav. (kW)	≈ 10	265	50
CW Beam current (mA)	<10	100	> 500
Parameter	Rossendorf ELBE FEL	XFEL (VUVFEL)	Cornell ERL injector
No. of cavities	2	8	5
Frequency (GHz)	1.3	1.3	1.3
Cells	9	9	2
HOM damping	Loop coupler	Loop coupler	Beam pipe absorber
Duty factor	CW	1%	CW
Temperature (K)	2.0	2.0	2.0
E_{acc} (MV/m)	10	28 (design)	5–15 (design)
Dynamic 2K heat load (W)	<100 (strong FE)	≈ 10	<21
Input coupling	Coaxial	Coaxial	Coaxial
Loaded Q	1.2×10^7	4.6×10^6	5×10^4 to 4×10^5
Peak RF power per cav. (kW)	10	≈ 150	100
CW RF power per cav. (kW)	10	≈ 2	100
CW beamcurrent (mA)	1	≤ 1	100 (design)

dynamic losses from the accelerating cavity mode to the helium bath are also of great importance because ERLs operate CW. This becomes particularly important for GeV class ERLs.

The following is a discussion of some of the parameters that impact the above considerations:

3.1. Cavity frequency

The main $\beta = 1$ SRF systems that are available or that are being planned operate at 1.5 GHz (CEBAF), 1.3 GHz (TESLA, Cornell ERL), 750 MHz (CEBAF injector), 704 MHz (BNL) and 500 MHz (Cornell, KEK).

An upper bound on the frequency is given by the need to limit the amount of HOM power being excited. This favors lower frequency systems, since the longitudinal loss factor of a cavity is proportional to $1/(\text{iris radius})^2$, and for a given cell shape the iris radius is proportional to $1/f$. Hence it is not surprising that the BNL electron cooler, being an ampere class machine, is planned for 704 MHz. Similarly the new 1A TJNAF cryomodules are also planned to operate at 750 MHz. On the other hand, 100 mA machines need not to operate below 1.3 GHz, and advantages of the higher frequency can be made use of.

As the frequency of cavities is lowered, the BCS losses decrease at a given operating temperature so that the power dissipation per meter acceleration is decreased. In principle 500 MHz, or even lower frequency, systems therefore appear most desirable. A lower bound on the frequency is given by the fact that the total losses eventually are dominated by the temperature independent residual losses. It is also important that the high- Q behavior can be maintained at the full operating gradient, which for most ERLs is in the range 15–20 MV/m. Results achieved with the Cornell and KEK 500 MHz system have demonstrated that at these fields anomalous, non-quadratic, losses (primarily field emission) do dominate so that the improvement gained by lowering the frequency is all but lost [1,2]. This is simply a result of the fact that the size of the cavity scales inversely with the frequency and large cavities are difficult to clean reliably. Therefore, given the present level of preparation technology, 700 MHz cavities represent a lower bound for the frequency of ERL cavities; this is sufficient to realize ampere-class ERLs. Fig. 2 demonstrates the influence of the non-BCS surface resistance on the AC power consumption of the cryoplant for selected cavity frequencies. Cavities in state-of-the-art SRF modules show a typical residual resistance of several

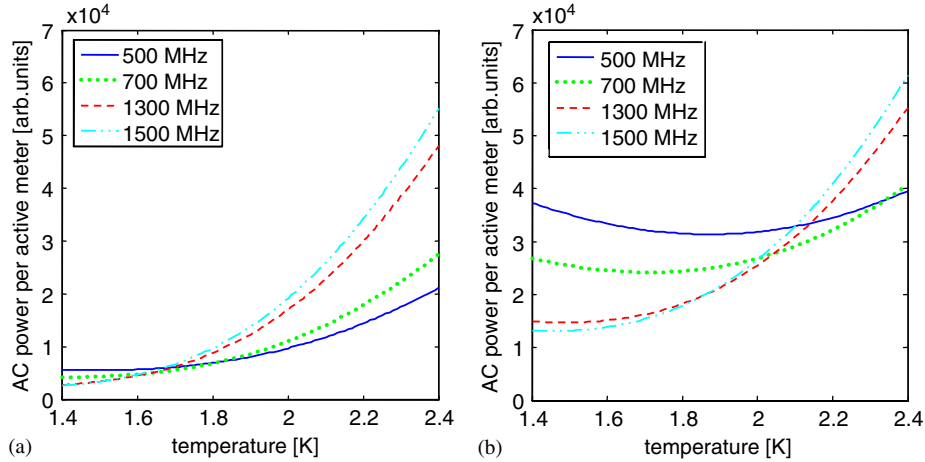


Fig. 2. AC power consumption per active length as function of temperature for selected cavity frequencies. The temperature dependent Carnot efficiency of the cryoplant is included. (a) With ideal 1 nΩ residual resistance. (b) With linac state-of-the-art 7 nΩ residual resistance.

nΩ. This favors the use of cavities above 1 GHz, operated below 2 K to minimize dynamic losses (see also Section 11). Future improvements in cavity-preparation technology as well as in cryomodule design will however shift this optimum to lower frequencies.

These considerations are particularly important for larger ERL projects where cost optimization is critical. For smaller projects, the available infrastructure (cavity preparation installations, RF sources, etc.) will probably dominate the choice of frequency.

3.2. Number of cells and cell-to-cell coupling

The number of cells and the cell-to-cell coupling is primarily determined by the requirement that the HOMs be extracted efficiently. In particular for 1 A class machines, external Q factors of order 10⁴ or lower must be achieved. This favors a small number of cells and a large iris radius. As an added benefit, the tunability of the cavity is also improved, although tuning procedures are well developed and no longer limit the number of cells up to order 10.

Fig. 3 depicts one example of a higher order mode in a multicell cavity. As the number of cells is increased the field at the end cells becomes weaker. Since HOM couplers invariably are located beyond the end cells these couple more and more weakly to the HOMs as the number of cells is increased, until eventually the damping becomes insufficient. The use of different shapes for the two end-cells can be help to extract the most dangerous HOMs to one side or the other, but this only works for a limited number of modes (e.g., TESLA).

In summary, easier HOM extraction is guaranteed by use of a larger iris radius and fewer cells. Ampere machines such as the BNL electron cooler thus use fewer (5) cells with a larger iris, whereas lower current machines can employ seven or even nine cells, with a smaller iris.

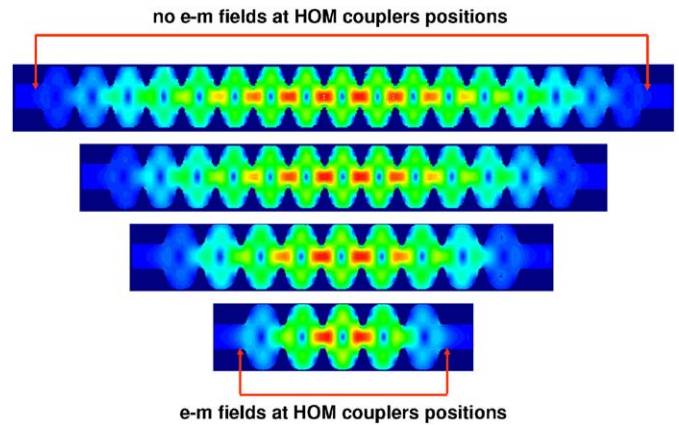


Fig. 3. Field distribution of a higher-order mode in a multicell cavity with changing number of cells. Lighter gray indicates higher fields. Courtesy of J. Sekutowicz.

3.3. Cavity shape

Much optimization is achieved through the design of the cavity shape. In the recent years, several new cell designs have been proposed, optimized for various applications, see Table 3. Optimization goals for example include low magnetic surface fields, low cryogenic losses, strong HOM damping, or low loss factors. Some of these objectives are mutually exclusive. Since the required gradients of 15–20 MV/m are moderate by present day standards, the overriding design criteria are HOM power generation/extraction (for high current) and cryogenic losses (for CW operation). Fig. 4 depicts three cavity shapes to illustrate this fact. The overriding design criteria for the 704 MHz BNL electron-cooling cavity, as in Fig. 4(a), is the need to extract kW of HOM power at 1 A beam current. For this reason the iris is enlarged to improve the cell-to-cell coupling to about 3%, and to lower the cell’s loss factor. Also the beam tube is large so that all modes will propagate

Table 3
RF parameters of different cell shapes. Courtesy of J. Sekutowicz

Parameter	Units	RIA	SNS	SNS	CEBAF Original cornell	CEBAF High gradient	CEBAF Low loss
β	—	0.47	0.61	0.81	1	1	1
f_0	(MHz)	793.0	792.8	792.8	1448.3	1468.9	1475.1
f_π	(MHz)	805.0	805.0	805.5	1497.0	1497.0	1497.0
k_{cc}	(%)	1.52	1.52	1.52	3.29	1.89	1.49
E_{peak}/E_{acc}	—	3.28	2.66	2.14	2.56	1.96	2.17
B_{peak}/E_{acc}	(mT/(MV/m))	6.51	5.44	4.58	4.56	4.15	3.74
R/Q circ. def.	(Ω)	28.5/2	49.2/2	83.8/2	96.5/2	112/2	128.8/2
G	(Ω)	136	176	226	273.8	226	280
$R/Q \times G$	(Ω^2)	2876/2	8659/2	18939/2	26421/2	29792/2	36064/2
k_\perp ($\sigma_z = 1$ mm)	(V/pC/cm ²)	0.15	0.13	0.11	0.22	0.32	0.53
k_\parallel ($\sigma_z = 1$ mm)	(V/pC)	1.19	1.25	1.27	1.36	1.53	1.71

Parameter	Units	RHIC Cooler	ILC Original TTF	ILC Low loss	ILC Reentrant large iris	ILC Reentrant small iris
β	—	1	1	1	1	1
f_0	(MHz)	683	1278.0	1281.5	1273.0	1278.5
f_π	(MHz)	703.7	1300.0	1300.0	1300.0	1300.0
k_{cc}	(%)	2.94	1.9	1.43	2.08	1.67
E_{peak}/E_{acc}	—	1.98	1.98	2.17	2.20	2.4
B_{peak}/E_{acc}	(mT/(MV/m))	5.78	4.15	3.7	3.9	3.5
R/Q	(Ω)	80.2/2	113.8/2	130/2	120/2	136/2
G	(Ω)	225	271	280	277	283
$R/Q \times G$	(Ω^2)	18045/2	30840/2	36400/2	33240/2	38600/2
k_\perp ($\sigma_z = 1$ mm)	(V/pC/cm ²)	0.02	0.23	0.38	0.23	
k_\parallel ($\sigma_z = 1$ mm)	(V/pC)	0.85	1.46	1.72	1.45	

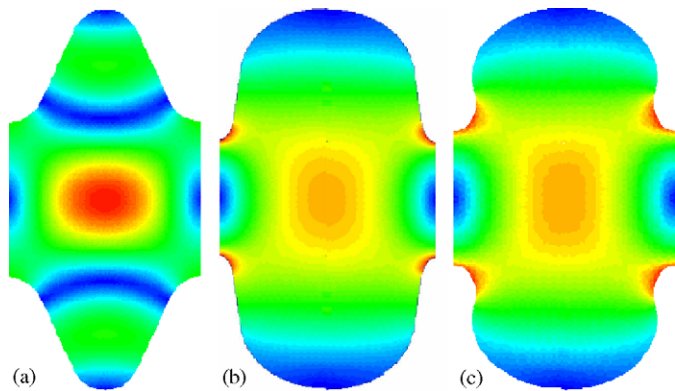


Fig. 4. Cavity shapes: (a) BNL electron-cooler cavity. (b) CEBAF low loss shape. (c) Re-entrant cavity for the ILC.

to the ferrite beam tube absorbers. However, this design does sacrifice shunt impedance, but for a relatively small machine like the electron cooler this is not a primary concern.

If cryogenic losses are the overriding criterion, the cell's volume in the high-magnetic field region can be enlarged as in Fig. 4(b) and (c) to reduce the surface magnetic field. This improves the factor $R/Q \times G$. A smaller iris radius further increases the shunt impedance.

4. Cavity quality

Since ERLs operate CW, the operating gradient is primarily limited by the cryogenic load, especially for larger machines. At present, refrigeration plants up to about $P_{cryo} = 5$ kW are in operation (e.g., CEBAF, LHC). The AC power consumption in this case is on the order of 5 MW. Significantly larger cryoplants appear unreasonable, if only because of the excessive wall-plug power requirement.

Given a linac energy E_b and N_{cav} cavities operating at a voltage V_{acc} each, the total dynamic cryogenic load of a linac is given by

$$P_{cryo} = \frac{N_{cav} V_{acc}^2}{2R/Q \times Q_0} \tag{1}$$

where R/Q is the intrinsic shunt impedance of the fundamental mode (in circuit definition), and Q_0 is its unloaded quality factor. Since $N_{cav} = E_b/V_{acc}$ one can calculate the operating gradient

$$V_{acc} = \frac{P_{cryo} 2R/Q \times Q}{E_b} \tag{2}$$

which for a 5 GeV ERL with TTF-style cavities, and $P_{\text{cryo}} = 5 \text{ kW}$ evaluates to

$$\begin{aligned} V_{\text{acc}} &= 10.4 \text{ MV/m} \quad \text{if } Q_0 = 10^{10} \\ V_{\text{acc}} &= 20.8 \text{ MV/m} \quad \text{if } Q_0 = 2 \times 10^{10}. \end{aligned} \quad (3)$$

Thus, even if high Q_0 values can be achieved, operation at the state-of-the-art limit (about 35 MV/m for TESLA cavities) is not an option for ERLs. Rather, the primary focus is on improving the cavity quality at lower gradient, typically in the range 15–20 MV/m.

Fig. 5(a) depicts a Q_0 measurement that achieved a quality factor above 10^{11} in a 1.5 GHz single-cell cavity, thereby demonstrating that very high Q_0 factors are intrinsically possible. Such cavity performance would permit the Cornell ERL to operate with less than 500 W of refrigeration power at 20 MV/m, although at 1.6 K. However, such results have yet to be reproduced consistently and in multicell cavities in real cryomodule environments. Fig. 5(b) shows for example the performance of an entire state-of-the-art cryomodule, with a Q_0 value of about 10^{10} at 20 MV/m at an operating temperature of 2 K. No field emission was detected at ERL typical operating gradients of 15 to 20 MV/m, demonstrating that these gradients are reasonable for future ERLs. Further dedicated tests of whole cryomodules at different temperatures are required to study the achievable medium field Q_0 in detail. A number of factors can impact the achievable Q_0 . These include

Material. The quality of the material impacts the cavity performance strongly, especially the maximum field that can be achieved. RRR 300 niobium has become the standard, with higher RRR values often produced by post-purifying the cavity at around 1400 °C. This improves the thermal conductivity of the material which in turn safeguards against quenches due to normal-conducting defects. An Eddy-current scan or newer techniques based on SQUID scans of the delivered sheets can detect such

defects in the niobium before it is used for cavity production.

Cavity preparation. Numerous techniques for cavity preparation exist [3]. These include an initial decrease, chemical etching with BCP (HF, HNO₃ and H₃PO₄, usually in a ratio of 1:1:1 or 1:1:2) or electropolishing, followed by high-pressure water rinsing, and heat treatment at 600–1400 °C for hydrogen degassing or post purification, respectively. These steps may have to be repeated several times. A final “treatment” may include in situ baking at around 120 °C for 24 h. Recent evidence has shown that this improves the BCS losses and often removes the “high-field Q -slope” that frequently limits the cavity performance [4].

Magnetic shielding. It has been shown that a residual magnetic flux present at the cavity will be trapped when the cavity is cooled through the transition temperature. This results in a residual resistance of about 0.35 nΩ per mG of trapped flux at 1.5 GHz [5]. Clearly, the earth’s field must be adequately shielded to achieve high Q_0 factors. For a typical cavity with a geometry factor of 270 Ω one must

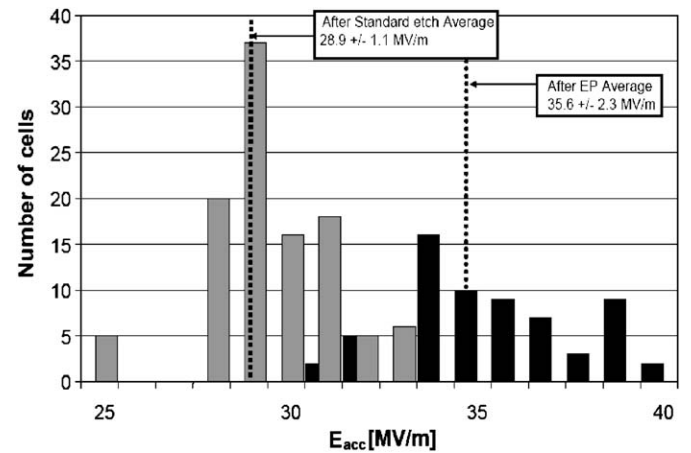
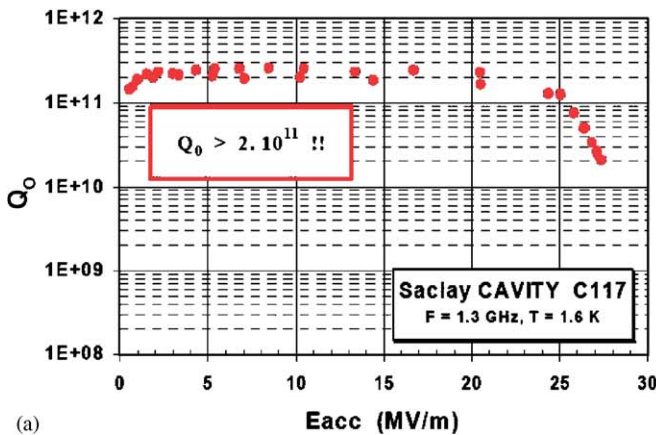
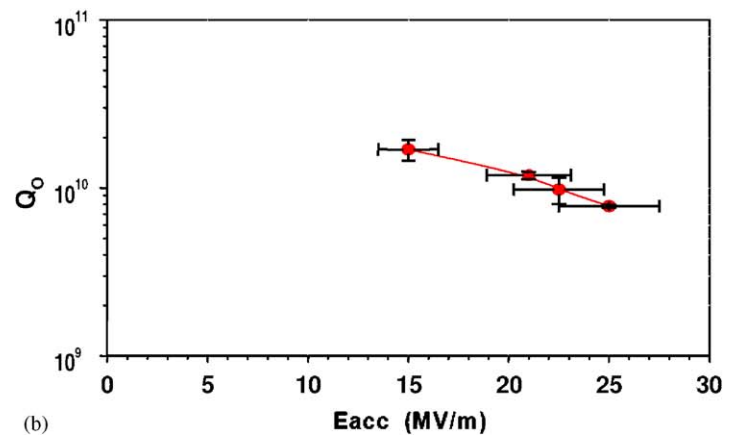


Fig. 6. Comparison of the maximum field reached for BCP-treated cavities with that of EP-treated cavities. Courtesy of DESY.



(a)



(b)

Fig. 5. (a) Single-cell 1.5 GHz cavity tested vertically at 1.6 K at Saclay. Courtesy of Saclay. (b) Integral TTF/VUVFEL module performance at 2 K (with eight 9-cell cavities). Courtesy of DESY.

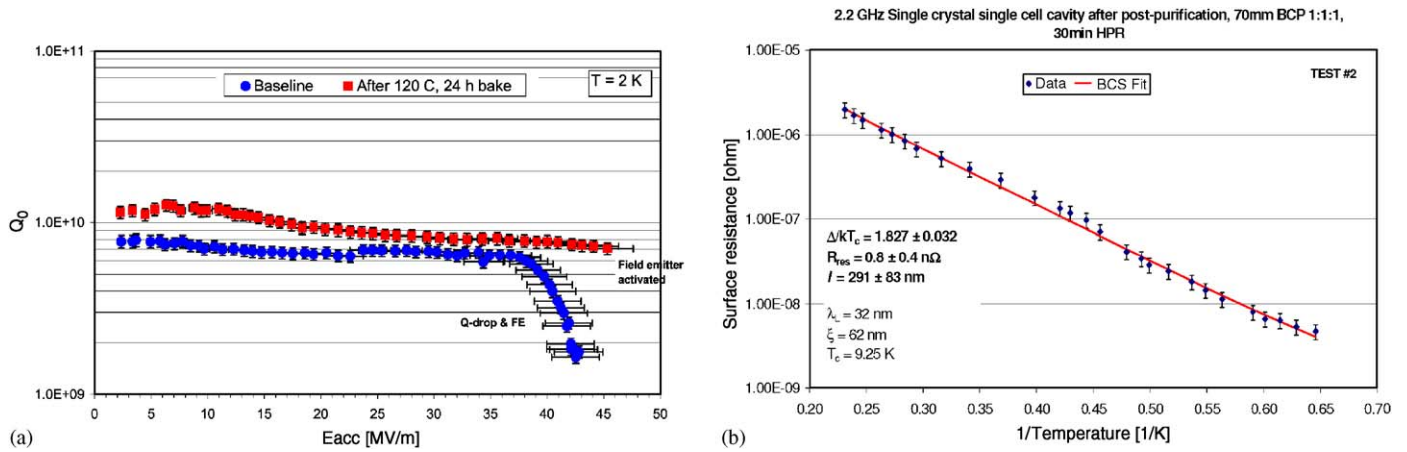


Fig. 7. Vertical test of a 2.2 GHz single crystal cavity. Note that the Q factors here are lower at 2 K than for 1.3 GHz because the BCS losses increase with frequency. Courtesy of P. Kneisel.

therefore achieve a shielding factor of at least 20 to assure a Q_0 of 3×10^{10} , even assuming there are no other loss mechanism.

Cavities performing at more than 25 MV/m require RRR 300 niobium that is post-purified to improve its thermal conductivity. Also, it has been demonstrated that electropolished (EP) cavities generally achieve higher fields than BCP treated cavities. Fig. 6 depicts one set of such measurements, the improvement due to EP being of order 6 MV/m. These cavities also suffer less from the high-field Q -slope provided a low-temperature bake is performed.

Still, even well prepared BCP cavities made from RRR 300 niobium achieve the 15–20 MV/m required for ERLs (see Fig. 6). In this range, EP treated cavities do not show any improvement in Q_0 over BCP treated ones. Therefore, EP treatment can be omitted for most ERL applications. To limit the chance of quenches due to inclusions, pre-production sheet scanning should however be carried out. Hydrogen de-gassing at about 600–800 °C is also recommended because fast cool downs, which can avoid the Q -disease in case of hydrogen contamination, are usually not possible in an accelerator environment.

Whether a low temperature bake at 130 °C for 48 h has any beneficial effect on the cavity Q_0 around 20 MV/m (BCP cavities) must still be determined. Here dedicated experiments are required.

A very important aspect appears to be the magnetic shielding. Especially for systems where the shield is cold it is difficult to predict what the residual field will be. In this case cryoperm, which has a high permeability at cryogenic temperatures, must be used. Only limited magnetic field measurements have been performed in realistic cryomodules and further measurements on cryomodules in the accelerator tunnel are a high priority to determine whether the current level of magnetic shielding is adequate for Q factors in the range of a few 10^{10} . A promising new cavity production technique is based on the use of “single” crystal sheets of niobium, cut directly from the ingot following e-

beam melting [6]. Several benefits are expected. The production of cavities may be less expensive, because costly rolling of sheets can be avoided. A very smooth surface, even when etched with BCP, is produced which may be easier to clean with high-pressure rinsing. First tests of such cavities have been very promising (see Fig. 7) reaching high-fields at a high Q_0 factor with very small residual surface resistance, but further research is needed to determine the suitability of single-crystal cavities for ERLs.

5. HOM damping

Future ERLs will operate with high currents up to 1 A, thus making strong HOM damping essential. Requirements on the damping of monopole and dipole modes result from the following effects:

- The average monopole HOM power per cavity is proportional to the longitudinal loss factor k_{\parallel} of the cavity, and is also proportional to the beam current I_b times bunch charge Q_b : $P_{\text{avg}} = k_{\parallel} I_b Q_b$. Note that the average power does not depend on the loaded Q of the HOMs. However, this power is significant in high current ERLs (of the order of hundreds of W to several kW), and thus needs to be intercepted at a well controlled point with good cooling efficiency. Since the longitudinal loss factor is proportional to $1/(\text{iris radius})^2$, 1 A ERLs use cavity frequencies below 1 GHz.
- If a beam spectrum frequency lines up with a monopole HOM frequency, resonant mode excitation occurs. In this case the power deposited in this HOM is given by $P_{\text{HOM}} = 2Q_L(R/Q)I_b^2$, being proportional to the loaded Q of the excited HOM, and to the beam current squared. For high currents this power can be very large, unless the mode has a low quality factor. This effect might be the most demanding one on HOM damping for high current ERLs.

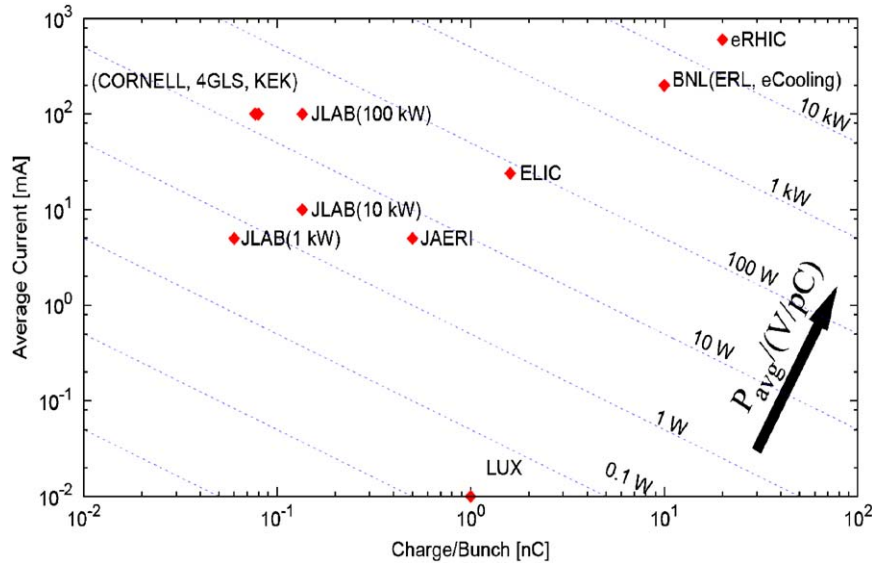


Fig. 8. Average monopole HOM losses normalized to 1 V/pC loss factor for selected ERL beam parameters.

- Dipole modes can cause beam-break-up (BBU) instability, if not sufficiently damped. The BBU threshold is proportional to $1/(R/Q \times Q)$, so again strong HOM damping is required to push the threshold above the operating beam current.

Fig. 8 shows the beam current/bunch charge parameter space for existing and planned ERLs. As discussed above, high current, high bunch charge ERLs will generate large amounts of HOM power, unless the longitudinal loss factor is kept small. The shown combinations of beam currents and bunch charge are not new for SRF applications. Storage rings like CESR (up to 800 mA, 20 nC) and KEKB (>1 A) operate at similar parameters, and are driven by single-cell SRF cavities. The new challenges in ERLs are however, that multi-cell cavities have to be used in the main linac for cost reasons, and that the bunch length in an ERL is significant shorter. While the mentioned storage rings have a bunch length of the order of 1 cm, the bunch length in an ERL is in many designs less than 1 mm. Accordingly the beam spectrum extends to significant higher frequencies (tens of GHz), and the HOM damping scheme needs to be adjusted for that.

Several methods for HOM damping have been developed and used in the past, see Fig. 9. Lower frequency modes (below some GHz) can efficiently be damped by HOM coaxial couplers. However, this type of damping does not work at high frequencies. High frequency and broadband HOM absorption is achieved by ring absorbers in the beam pipe, where the beam pipe diameter is enlarged (e.g. KEKB cavity, Cornell ERL, BNL ERL) or a fluted beam pipe (e.g. CESR cavity) is used to propagate all potential dangerous HOMs to the absorber down the beam pipe. Broadband damping is also achieved by means of waveguide HOM couplers (e.g. CEBAF cavity) and a beam pipe coaxial design (e.g. KEKB crab cavities). All of these

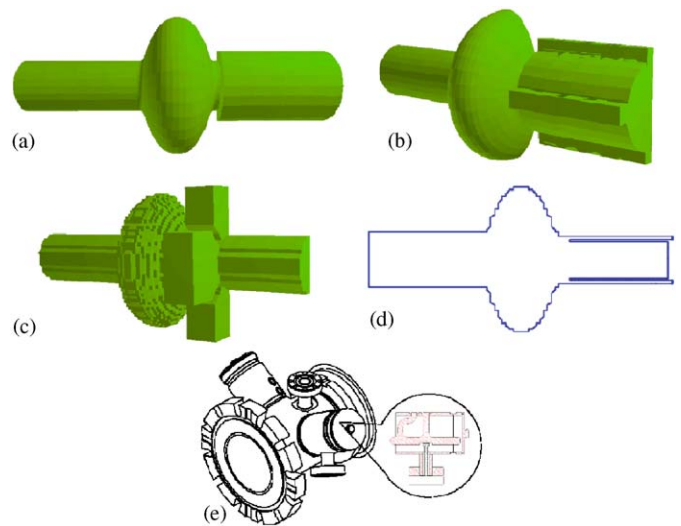


Fig. 9. Methods of HOM damping: (a) Enlarged beam pipe. (b) Fluted beam pipe. (c) Waveguide dampers. (d) Coaxial/radial beam pipe. (e) HOM coaxial loop coupler.

methods can provide strong and broadband HOM damping, see Fig. 10(a). The influence of the cell shape on HOM damping can be seen from Fig. 10(b). Though some differences exist (about a factor of three), for 100 mA class ERLs the cell shape can be optimized for low dynamic cryogenic losses without trading HOM damping beyond an acceptable limit. Fig. 11 finally shows that HOM impedances do increase with the number of cells per cavity, but this increase is less than quadratic with respect to the cell number. This demonstrates, that multi-cell cavities are feasible for ERL main linacs, with the number of cells decreasing as the beam current increases.

In all broadband damping concepts, the HOM power is absorbed by RF lossy materials. These materials are

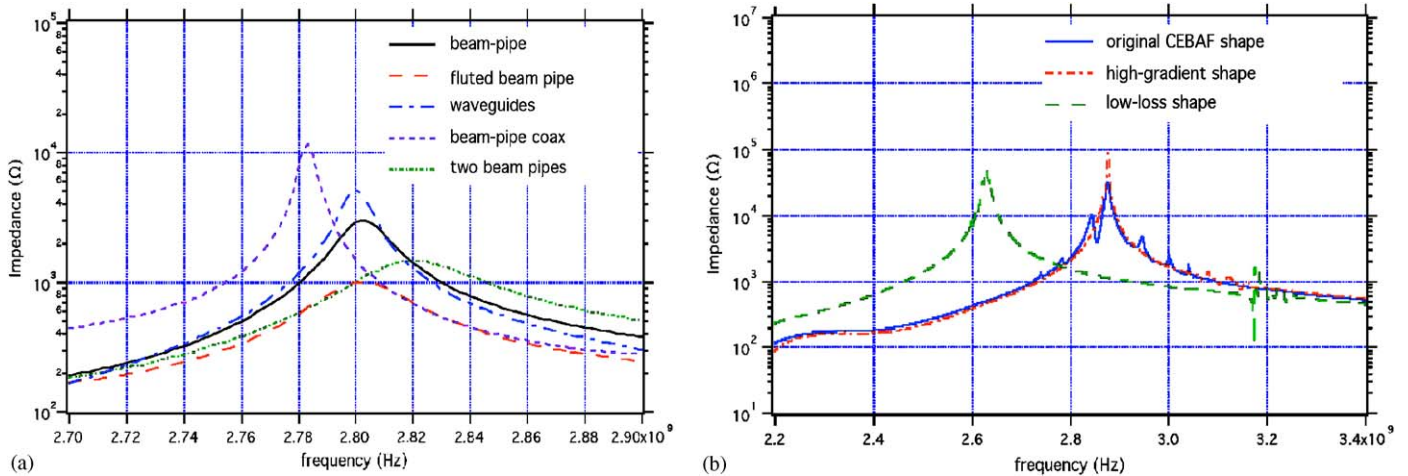


Fig. 10. (a) Calculated TM011 mode impedance with various damping schemes (single-cell 1.5 GHz cavity of original CEBAF shape). (b) Calculated TM011 band impedances with different cavity shapes (7-cell cavity with beam-pipe damping). Courtesy of B. Rimmer.

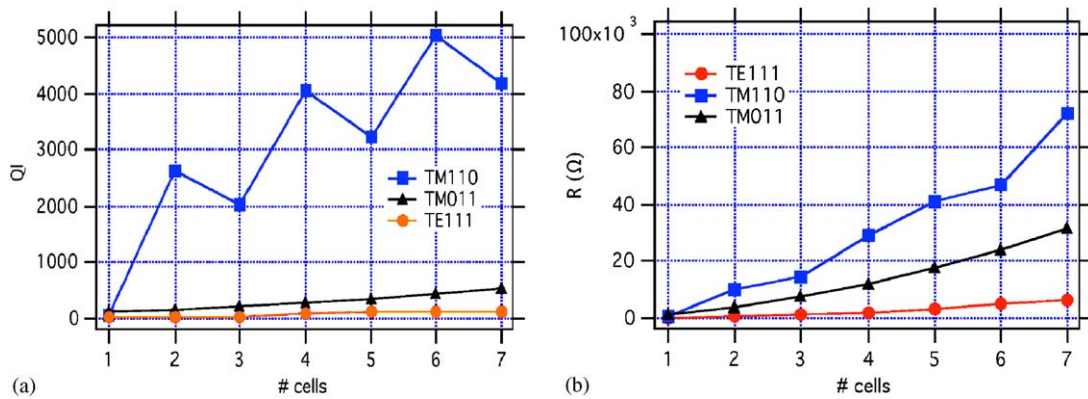


Fig. 11. Impact of number of cavity cells on HOM impedance (TM011, TE111 and TM110 passband modes with beam pipe damping). (a) Loaded Q vs. number of cells. (b) Impedance vs. number of cells (dipoles at 25 mm transverse offset). Courtesy of B. Rimmer.

usually placed at a temperature between about 70 and 300 K for good cooling efficiency. Detailed studies have been done to measure the RF properties of the materials over a wide frequency range and at cryogenic temperatures [7].

Simulations have become a powerful tool in designing HOM damping for SRF cavities. Three-dimensional models allow to study HOMs and their damping in detail. The two 100 mA ERL injectors presently under construction (see Section 12) will provide a valuable opportunity to cross-check these simulations with reality.

6. Microphonics

“Microphonics” refers to the detuning of an RF cavity by external sources like ground vibrations or LHe bath pressure fluctuation. These vibration sources can couple to the cavity via multiple paths. It is useful to distinguish between random noise and defined frequency vibrations. When a vibration source frequency lines up with a mechanical resonance of a cavity, particularly strong microphonics can occur.

Maintaining low cavity microphonic levels is of the utmost importance for an ERL. The main linac cavities have virtually zero beam-loading, and so for efficient cavity operation they should be operated at a very high loaded quality factor Q_L . The optimal Q_L is solely determined by the ratio of the fundamental mode frequency f_0 and the cavity peak detuning Δf

$$Q_{L,optimal} = \frac{1}{2} \frac{f_0}{\Delta f}. \tag{4}$$

The minimal required RF peak power to maintain a constant RF field in amplitude and phase in a zero beam-loading cavity detuned by Δf is given by

$$P_{g,minimal} = \frac{V_{acc}^2}{2R/Q} \frac{\Delta f}{f_0}, \tag{5}$$

where V_{acc} represents the accelerating voltage of the cavity and R/Q is the intrinsic impedance of the fundamental cavity mode (circuit definition). It should be pointed out that the minimal required RF peak power is directly proportional to the maximum peak detuning. In designing an ERL, it is therefore extremely important to have a good

estimate of the peak cavity detuning when determining the required RF peak power. If one underestimates the peak detuning, and thus the installed RF power is not sufficient, the RF source will run against its maximum output power, and so the cavity is likely to trip every time the cavity detuning exceeds the estimated peak detuning.

Most existing high- β superconducting RF machines have significant beam loading. Because of the resulting relatively high fundamental mode bandwidth (typically between 100 Hz and a few 1 kHz), microphonics is of lesser concern in such machines. Accordingly only limited effort has been made in the past in measuring microphonics, understanding its sources, and improving the mechanical design of the cavities and cryostat to minimize microphonics. Table 4 summarizes measured rms microphonics levels for different superconducting machines. Following [8], the peak cavity detuning is estimated as 6σ . In all cases significant fluctuation in microphonics has been found from cavity to cavity, even within the same cryomodule. The reason for this is not well understood. Also in all cases

the dominating part of the microphonics occurs at vibration frequencies below 400 Hz, see Fig. 12 for examples.

Table 4 shows that proof-of-principles for low microphonics SRF cryomodules exists, with a peak detuning below 10 Hz appearing realistic. However, the fluctuation in microphonics level from cavity to cavity as well as temporal changes in the microphonics amplitude need to be investigated in much greater detail on large SRF installations. Likewise the sources of microphonics as well as their coupling to the cavities should be studied in more detail. This knowledge would allow to improve the mechanical design of the cryostat and the cavities for lower microphonic levels in future SRF installations. A further open question is how much microphonics is correlated between cavities within a single cryomodule and between cryomodules in a large SRF machine. In the case of correlation, the field perturbations caused by microphonics are also correlated. This would have major impact on the achievable beam energy stability, since only in the case of non-

Table 4
Measured microphonic levels

Machine	σ (Hz)	6σ (Hz)	Comments
CEBAF	2.5 (average)	15 (average)	Significant fluctuation between cavities
ELBE	1 (average)	6 (average)	
SNS	1–6	6–36	Significant fluctuation between cavities
TJNAF FEL	0.6–1.3	3.6–7.8	Center cavities more quiet
TTF	2–7 (pulsed)	12–42 (pulsed)	Significant fluctuation between cavities

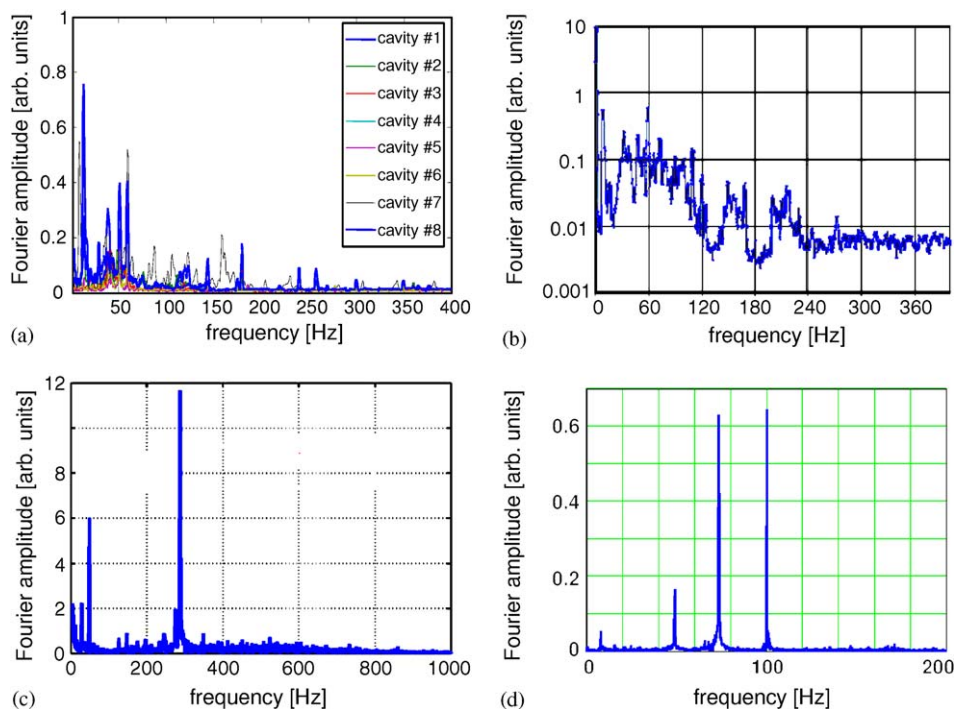


Fig. 12. Examples of microphonics spectra. (a) TJNAF FEL (CEBAF upgrade module). (b) SNS module. (c) TTF test cryostat (CHECHIA). (d) ELBE module.

correlation is the energy fluctuation suppressed by the factor $1/\sqrt{\text{number of cavities}}$.

Besides designing the cryomodule for minimal microphonics, a further reduction in microphonics amplitude could potentially be achieved with active control schemes, making use of a fast frequency tuner. Initial studies have shown promising results [9,10]. However, it should be pointed out that active microphonics compensation is challenging, and must be supported by a good mechanical design of the cavity and its surrounding hardware.

In conclusion, low microphonics amplitudes have been demonstrated in real machine environments giving an optimal loaded Q of above 5×10^7 . Further reduction of microphonics by active and passive damping schemes appears feasible.

7. Frequency tuner

Because of the small bandwidth of ERL main linac cavities, fine frequency control and good frequency stability are mandatory. The frequency tuner needs to provide sufficiently fine resolution (<1 Hz), small backlash, and high stiffness. Several cavity frequency tuner have been developed over the last years; see Table 5 for examples. These existing and tested tuner designs can be adopted for ERLs, possibly with minor modifications. Since reducing microphonics is of major importance for ERLs (see Section 6), the tuner and LHe vessel should be designed for high stiffness with mechanical resonances only at high frequencies (several 100 Hz). Before application to an ERL, the existing frequency tuner designs should be studied with respect to their mechanical properties, and eventually improved. Experience has shown that the driving stepping motor can be placed inside the cryomodule at cryogenic temperature, though long-term reliability and maintainability is still a concern in some cases. Therefore, smaller linac installations tend to place the motor outside of the vacuum vessel. To improve maintainability of a cold motor inside of the vacuum

vessel, the SNS and the Cornell ERL injector modules have access ports in the vessel, allowing to reach the motors without dismantling the whole module.

All recent tuner designs have integrated fast frequency tuners (piezo-actuated or magnetostrictive) for fine and fast frequency control. This feature in principle allows to compensate cavity microphonics. However, the required control algorithms are quite complex, and only first steps in developing a controller have been made so far [9,10]. The achievable performance of active microphonics control will significantly depend on the mechanical design of the cavity-vessel-tuner assembly, and on what part of the microphonics is deterministic rather than stochastic. In several tuner designs the fast actuator is placed inside the vacuum vessel at cryogenic temperature. The resulting reduced stroke of a piezo-actuator and reliability issues have been studied in detail [11].

8. RF control

All ERLs require very stable RF fields, and ERL light sources will require the highest field stability, of the order of 10^{-4} in relative amplitude and well below 0.1° in phase. This alone is challenging, and is made even more demanding by the fact that the superconducting cavities in an ERL need to be operated with a high loaded Q_L of several 10^7 , possibly up to 10^8 , for efficient operation.

This combination is challenging for the Low-Level RF (LLRF) systems for the following reasons:

- At a loaded Q_L of several 10^7 – 10^8 the cavity bandwidth is only a few 10s of Hz, while the Lorentz-forces will detune the cavities by several hundred Hz during cavity filling. It is therefore essential to compensate for the Lorentz-force detuning very precisely during cavity turn-on.
- The small cavity bandwidth also makes the RF field in the cavity extremely sensitive to any perturbation of the cavity resonance frequency due to microphonics. At the

Table 5
Frequency tuner parameters. Courtesy of E. Daly

Parameter	CEBAF Original	CEBAF Upgrade SL21	CEBAF Upgrade renaissance	RIA $\beta = 0.47$	SNS $\beta = 0.81$	ILC Original	ILC Blade tuner
Coarse range (kHz)	± 200	± 200	± 400	950	± 220	± 220	± 250
Coarse resol. (Hz)	NA	< 2	2–3	< 1	2–3	< 1	< 1
Backlash (Hz)	≥ 100	< 3	< 3	NR	< 10	NR	NR
Fine actuator	Non	Piezo (150 V)	Piezo (1 kV) or magnetostr.	Piezo (100 V)	Piezo (1000 V)	Non	Under design
Fine range (Hz)	—	> 550	1200 (piezo) 30 kHz (magnet.)	11 000	> 2500	—	> 1000
Tuning dir.	Tens & compr.	Tension	Tension	NA	Compr.	Tens & compr.	Tens & compr.
Mechanism	Immersed	Vacuum	Vacuum	Vacuum	Vacuum	Vacuum	Vacuum
Drive	Warm	Warm	Cold	Warm	Cold	Cold	Cold

optimal loaded Q_L (see Eq. (4)) the peak detuning is equal to the HWHM bandwidth of the cavity, causing significant field perturbation. This challenge is amplified by the fact that future ERL light sources will require very tight field stability in both amplitude and phase. Fortunately, for higher frequency perturbations the increased field sensitivity is partly compensated by the increased low pass characteristic of the high Q_L cavity.

- In generator driven LLRF systems, Lorentz-force detuning and field amplitude fluctuations can cause an unstable feedback loop (so-called ponderomotive instability). The smaller the cavity bandwidth the higher is the risk of this instability, and high field stability is essential to suppress this type of instability.
- Ideally the beam loading of the accelerated beam and the decelerated beam in an ERL cancel perfectly. In reality, however, small phase fluctuation of the beams and beam current fluctuations will result in a varying beam loading. The resulting field perturbations needs to be compensated by the field control system while only limited RF drive power is available.

These challenges explain why the highest loaded Q_L at which elliptical RF cavities in linacs are operated presently is limited to Q_L of $1\text{--}3 \times 10^7$. However, as discussed above, operating the cavities in an ERL at even higher Q_L is highly desirable for most efficient operations. Table 6 gives examples of existing LLRF systems. All new large scale LLRF systems are based on digital controllers. Recent progress in digital hardware makes a digital approach the option of choice because of its superior flexibility. Fast Field Programmable Gate Arrays (FPGA) allow for minimal latency in the digital control loops, so that in most cases latency of the digital hardware is no longer a limiting factor.

Two ERL-specific LLRF challenges need to be addressed: (1) the compensation of the varying beam loading, and (2) the operation at highest loaded Q_L . The later challenge has been studied in detail at the TJNAF FEL in a collaboration between LEPP and Jefferson Lab. In a

proof-of-principle experiment, Cornell's newly developed digital LLRF system [12,13] has been connected to one of the FEL 7-cell cavities. This LLRF system includes the following features: low noise field I/Q detection, low latency field control, a feedback loop for the slow stepping-motor-driven tuner, advanced feedforward-feedback cavity frequency control with a fast piezo-driven frequency tuner, and a state-machine for start-up and trip-recovery. After an initial test at the standard $Q_L = 2 \times 10^7$, the loaded Q_L was increased to about 10^8 . Excellent field stability was achieved with full 5 mA beam current in energy recovery mode; see Fig. 13(a–c). Less than 500 W of driving RF power was required for operation at a gradient of 12.3 MV/m. No dependence of the field stability on beam current (0–5.5 mA) and off-crest angle (between -40° and $+40^\circ$) was found. Even at this high loaded Q_L the cavity operated very reliably over several hours without any trips. Piezo-tuner based frequency control proved to be very effective in keeping the cavity on resonance during cavity filling. The Lorentz-force detuning of the cavity is compensated by the piezo tuner, and thereby allows to ramp up reliably to high gradients in less than 1 s even at $Q_L = 1.2 \times 10^8$; see Fig. 13(d–e). This is desirable for fast trip recovery in a large ERL.

The described proof-of-principle test demonstrates that no fundamental limit prohibits the cavity operation at a loaded Q_L of 10^8 , and that high field stability is achievable at the same time. It should however be noted, that it is desirable to repeat this test with a higher beam current to fully study the impact of random beam loading in the ERL main linac cavities. Also, it is important to realize, that the required tight phase stability needs to be supported by a sufficiently stable reference RF signal generation and distribution.

9. Input couplers

The obvious purpose of couplers is to provide means of transferring power from a generator to a superconducting cavity. However, the first criteria for designing couplers are

Table 6
Examples of LLRF systems and achieved field stability

LLRF system	Type	Gradient (MV/m)	Beam cur. (mA)	Loaded Q	σ_A/A	σ_ϕ (deg)	Comment
SNS	Digital I/Q	<16	38	7×10^5	$<1 \times 10^{-2}$	<1	Pulsed
TTF	Digital I/Q	20–25	<10	2×10^6	$<1 \times 10^{-3}$	<0.1	Pulsed
CEBAF	Analog	<12	<1	7×10^6	$<1 \times 10^{-4}$	0.02	
ELBE	Analog	10	1	1×10^7	2×10^{-4}	0.03	
S-Dalinnac	Analog	≈ 5	≤ 1	3×10^7	1×10^{-3}	0.3	
CESR	Digital I/Q	<10	<800	2×10^5	1×10^{-3}	0.25	
Cornell at CEBAF	Digital I/Q	10	0.4	4×10^7	1×10^{-4}	0.02	High Q_L test
Cornell at TJNAF FEL	Digital I/Q	12	5	1×10^8	1×10^{-4}	0.02	High Q_L test

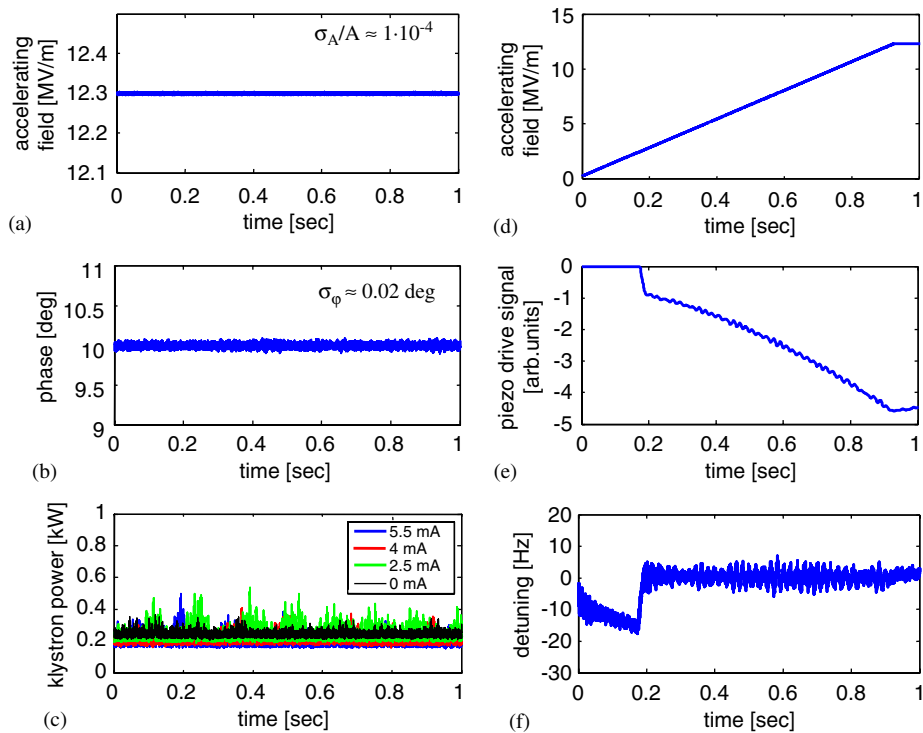


Fig. 13. Results from a test of Cornell's LLRF system at the TJNAF FEL with a high Q_L of 1.2×10^8 . (a–c) CW operation. (d–e) Cavity filling with piezo tuner based Lorentz-force detuning compensation [13].

that they do not compromise the performance of the cavities they are connected to, and that they shall not negatively affect the beam. For a low energy, small emittance beam this can result in the requirement that transverse on-beam-axis field must be avoided. Asymmetric input couplers can cause time dependent kick fields, which will result in emittance growth. In the Cornell ERL injector, for example, this effect is addressed by a twin-coupler design with vanishing transverse on-axis fields. While the power transfer in the main linac is moderate (typically on the order of 10 kW), in an ERL injector, high CW power handling by the input couplers is essential. As a matter of fact, the number of cells in the ERL injector RF and the field gradient in the cavities is often limited by the maximal RF power handling of the input couplers. Main features an input coupler must provide include appropriate transmission to the cavity, support of large thermal gradients and high RF power handling without transferring large amounts of heat to the cryogenic environment, and one or more vacuum barriers to atmospheric pressure. Simulations have become one of the most important tools in predicting the complex behaviors of couplers and have enormously improved reliability and shortened the time necessary to achieve successful design solutions. Such simulations include mechanical, thermal, electromagnetic, and multipacting studies.

A large number of waveguide and coaxial input couplers have been designed, built and tested over the years; see Table 7 for examples. Input couplers designs for the main

linac power levels are available for the whole ERL cavity frequency range. Several high CW power input couplers are presently under development for the ERL injector RF, e.g. for the TJNAF and Cornell 100 mA injectors.

A controversial question is, whether adjustable coupling is required. Adjustability is desirable for flexibility, but it increases the complexity of the coupler, and within some limits the coupling can also be changes by means of waveguide stub-tuners. For high energy ERLs, the cost of the input couplers becomes a critical issues, and improvements in both complexity and reliability are highly desirable.

10. RF power sources

ERLs require a large number of RF power sources. GeV scale machines have several hundreds of cavities, and each cavity is driven by its own power source. The one-source-per-cavity concept is essential, because the high loaded Q_L of the cavities prohibits vector sum control of multiple cavities; microphonics would cause intolerable large fluctuations of the individual fields in case of vector sum control. Requirements for the RF power sources include high efficiency, reliability and long life time, low pushing factors, and reasonable price. High linearity and high efficiency over the full output power range is also desirable. Two different types of RF power sources are used in ERLs: klystrons and Inductive Output Tubes (IOTs).

Table 7

Examples of high power input couplers (existing or under construction). Courtesy of S. Belomestnykh

Machine	Type	Frequ. (GHz)	Window	Q_{ext}	Max. power (kW)
LEP2	Coax. fixed	0.352	Cylindrical	2×10^6	CW: 565 (test, trav. wave) CW: 100 (operation)
LHC	Coax. variable (60 mm stroke)	0.400	Cylindrical	2×10^4 – 3.5×10^5	CW: 500 (test, trav. wave) CW: 300 (test, stand. wave)
PEP-II	WG fixed	0.476	Disk WG	7×10^3	CW: 500 (test, trav. wave)
CESR	WG fixed	0.500	Disk WG	2×10^5	CW: 450 (test, trav. wave) CW: 360 (operation)
HERA	Coax. fixed	0.500	Cylindrical	1.3×10^5	CW: 300 (test, trav. wave) CW: 65 (operation)
TRISTAN	Coax. fixed	0.509	Coax. disk	1×10^6	CW: 200 (test, trav. wave) CW: 70 (operation)
KEKB	Coax. fixed	0.509	Coax. disk	7×10^4	CW: 800 (test, trav. wave) CW: 380 (operation)
APT	Coax. variable (± 5 mm stroke)	0.700	Coax. disk	2×10^5 – 6×10^5	CW: 1000 (test, trav. wave) CW: 850 (test, stand. wave)
BNL ERL	Coax. fixed	0.704	Coax. disk	2×10^7	CW: 50 (design)
SNS	Coax. fixed	0.805	Coax. disk	2×10^5	Pulsed: 2000 (test, peak) (7.8% DC: 1.3 ms, 60 Hz) Pulsed: 1800 (TW, 1.3 ms, 2 Hz) CW: 4 (test, trav. wave)
TTF(3)	Coax. variable (17 mm stroke)	1.300	Cylindrical	1×10^6 – 2×10^7	CW: > 10 (test, TW, air cooled) CW: 75 (design)
Cornell ERL	Coax. variable (> 15 mm stroke)	1.300	Cylindrical	9×10^4 – 8×10^5	CW: 50 (test, trav. wave) CW: 30 (operation)
TJNAF FEL	WG fixed	1.500	Planar WG	$< 2 \times 10^7$	

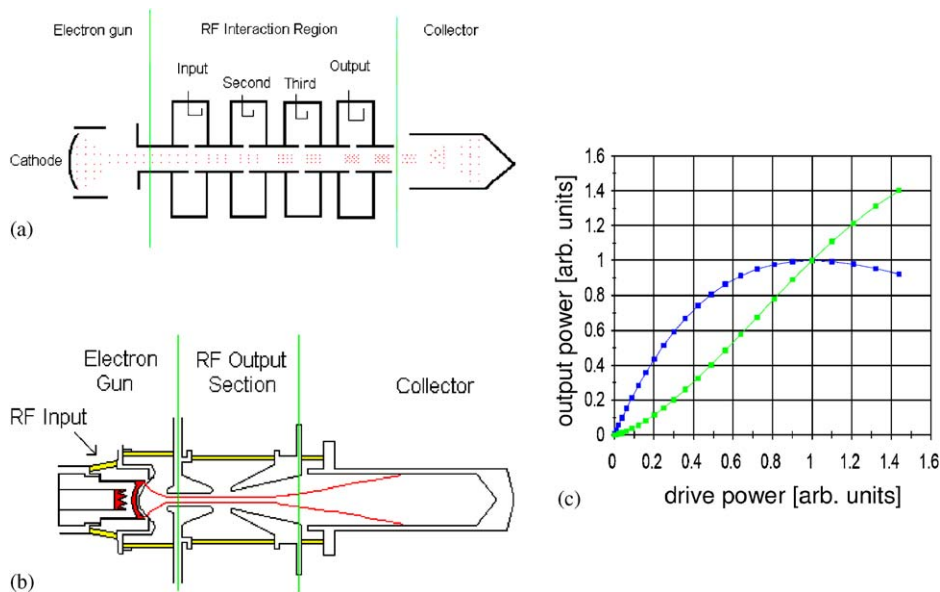


Fig. 14. (a) Schematic of a klystron. (b) Schematic of an IOT. (c) Characteristics of the output power vs. drive power for klystrons (black, saturating) and IOTs (gray, not saturating). Courtesy of CPI.

The klystron is an RF amplifier that uses velocity modulation of a DC beam of electrons to amplify the RF input. It uses several bunching cavities, which are usually integral to the klystron, as depicted in Fig. 14(a). If it is

operated at reduced power there is a rapid reduction in efficiency. At high drive powers, the output saturates, as shown in Fig. 14(c). This usually necessitates operating a klystron at 10–20% below saturation in order to provide

sufficient incremental gain for RF field control. Klystrons are high gain devices (typically >40 dB), and thus require only low drive power. They provide high efficiency if operated close to saturation, and are therefore a good option for the ERL injector RF with its constant RF power demand (constant beam loading). A variety of CW klystrons at different frequencies and power levels are available from industry, especially below 1 GHz. High power klystrons above 1 GHz are presently under development, e.g. a 150 kW, 1.3 GHz source for the Cornell ERL injector.

The IOT amplifier uses a grid to density modulate the electron beam, and so has no bunching cavities, making it a short device; see Fig. 14(b). This results in several advantages. First, IOTs have high efficiency, and the efficiency stays relatively high even if operated at reduced output power. Secondly, IOTs show high linearity, and therefore small pushing factors. Thirdly, they do not saturate and thus can be operated up to their maximum output power; compare Fig. 14(c). On the negative side, the gain of an IOT (typically 20–23 dB) is lower than a klystron, and a higher power drive amplifier is therefore required, which contributes significantly to the overall cost of an IOT-based RF transmitter. In addition, the grid geometry will not permit IOTs to operate at high frequencies like klystrons. While a number of IOTs are available at frequencies below 1 GHz (driven by the television market), only recently have 1.3 GHz IOTs been developed by industry, specially designed for particle accelerator applications. Because of their simplicity, IOTs should be a relatively inexpensive device, offsetting the higher cost of the drive amplifier. For the ERL main linac, IOTs are likely to be the option of choice because of their higher efficiency at reduced output power, as compared to klystrons. For example, present 1.3 GHz IOTs surpass 60% efficiency at full output power and still reach 35–40% efficiency at about half of the peak power. This becomes significant in the main linac RF, where the required drive power is determined by the cavity detuning due to microphonics and by random beam loading. Both effects are time varying, and as a result the maximum RF drive power will be required only occasionally, with the average RF power close to half of the peak power. Accordingly, main linac IOTs should be optimized for high efficiency at reduced power levels rather than at maximum power. Further optimization will be required to increase gain and efficiency while reducing the cost of the complete transmitter.

11. Cryogenics

Since ERLs operate CW, the dynamic heat load from the cavities is very significant. A GeV scale ERL, if operated at 2 K, has a heat load of several kW, resulting in a cryoplant power consumption in the order of several MW. Obviously, minimizing the cryoplant power consumption becomes essential for these ERLs. As discussed in Section

3, this can be done by optimizing the cell shape, and by operating the cavities below 2 K. However, the latter only works for cavities with low residual surface resistance, compare Fig. 2. Obviously, special care has to be taken in cavity preparation and cryomodule design (low residual magnetic fields) to achieve this, as is discussed in Section 4.

Operation below 2 K needs to be considered carefully, however. It has potential impact on the cryomodule design itself as well as the cryoplant. For a detailed discussion refer to Ref. [14].

The cryogenic piping in the module needs to be of sufficient diameter to support the high heat loads. This includes the heat conduction in the LHe vessel itself, and the mass flow through the module and the entire linac. Even heat flow through He-II is limited, and boiling should be avoided for stable operation and low microphonics. This requires the local temperature in the LHe bath to be below the saturation temperature, which is a function of pressure. As a rule of thumb, the heat flux per cross section in 1.8 K He-II needs to be less than $0.5\text{--}1\text{ W/cm}^2$, depending on tube shape and length. For the pump lines, pressure drop along the line and vapor velocity needs to be evaluated carefully. However, if the cryogenic layout is sized for 2 K operation, it should also allow operation at lower temperatures, as long as the cavity losses are still BCS dominated. This comes from the fact, that pressure drops, critical gas velocities, work of compression, and the lower gas densities at lower temperatures seem to be balanced by the lower cooling loads and the related lower mass flows. This in principle allows to optimize the operating temperature after an ERL has been built and the actual cavity performance is known.

If this is envisioned, special care has to be taken in the design of the cryogenic plant to support flexibility in operating temperature. For about each 0.2 K temperature drop, another cold compressor stage will be required. Thus, sufficient space needs to be available to add cold compressors at a later time. However, the additional cost for cold compressors is balanced by the smaller cryogenic loads, requiring fewer warm screw compressors, so that potentially the overall capital cost of the cryoplant does not depend significantly on the operating temperature. Note that this statement needs further evaluation and is only valid as long as BCS losses dominate in the cavities. Also, operation below 1.8 K needs further studies, since instabilities might occur. In any case, the design of a cryoplant should always include at least 50% overhead on all expected loads.

12. Injector cryomodules

In an ERL, the injector cryomodule needs to accelerate a “soft” low energy beam from an electron source while preserving its emittance. The energy gain in the injector RF should be high enough to make it suitable for injection into a main linac of an ERL, but low enough to avoid unnecessary waste of power. Note that the energy in the

injector is not recovered. Typically the required energy gain in the injector RF is in the range 5–10 MeV. The two major challenges which need to be addressed especially in the injector modules are:

- Significant amount of RF power needs to be transferred to the beam. As mentioned in Section 9, this requires high power handling by the input couplers, and usually results in short cavities (one to two cells) to limit the power per coupler.
- Optimization for emittance preservation is critical if very small emittance is required, e.g. in the Cornell ERL. This requires good HOM damping and very low transverse kick fields from beam pipe asymmetries and couplers.

These required features usually make the injector RF modules different from main linac ones. In other respects the requirements on the injector cryomodules are similar or relaxed in comparison to the main linac cryomodules. This often includes HOM damping, microphonics and tuner resolution, field control and cryogenic loads.

Two major projects are underway to develop special ERL injector modules for high current beams: the 100 mA injector for the TJNAF FEL, and the 100 mA injector for the Cornell ERL; see Table 2 and Fig. 1. The experience from these projects will also be very valuable in designing future cryomodules for ERL main linacs.

13. Transfer to industry

Only a small number of laboratories or institutes have the infrastructure and personnel to assemble whole SRF cryomodules, e.g. DESY and TJNAF. It is therefore likely, that industry will increasingly be asked in the near future to provide large sub-assemblies of SRF cryomodules or whole modules. Different approaches can be envisioned for this, and have successfully been applied to other large scale productions by industry for particle accelerators:

- Use of industry as job-shops or service supplier. In this case the required R&D and the design and performance risks remain by the laboratories or institutes. This approach is usually chosen for small quantities.
- Prototypes are developed by the laboratories or institutes, or jointly with industry. The established procedure and designs are then transferred to industry. The production is done in strong interaction with the laboratories or institutes, and the design and performance risks remains by the laboratories or institutes. The responsibility for faultless assembly is however with the vendors. A bonus might be offered, if certain performance specifications are surpassed.
- Prototypes are developed by the laboratories or institutes, or jointly with industry. The established procedure and designs are then transferred to industry. Production is done by industry with guaranteed

performance specifications. In this approach, proof by the laboratories or institutes that procedures are mature is necessary to enable industry to give guarantee for performance. This proof can mean significant effort, including the production and tests of complete SRF cryomodules.

- Prototypes are developed by industry. Production is done by industry with guaranteed performance specifications.

Obviously, each of these approaches has significant impact on cost, which needs to be evaluated carefully for each individual project.

14. Conclusions

SRF for ERLs is an very active, challenging, and exciting application of SRF technology. As discussed in this paper, several issues should to be addressed, before an fully optimized high current ERL can be built. The R&D path to address these issues within the next few years is clearly visible.

Acknowledgements

The contributions from many colleagues have made the SRF working group during the ERL 2005 workshop very productive. Their work and excellent presentations during the ERL workshop are gratefully acknowledged. Special thanks go to Mike Dykes as co-convenor of the working group.

References

- [1] S. Belomestnykh, et al., in: Proceedings of the 2005 Particle Accelerator Conference, Knoxville, TN, 2005.
- [2] T. Furuya, et al., in: Proceedings of the 1997 Particle Accelerator Conference, Vancouver, BC, 1997.
- [3] P. Schmueser, et al., Superconducting TESLA cavities, PRST—AB 3 (2000) 092001.
- [4] G. Ciovati, in: Proceedings of the 2005 Workshop on RF Superconductivity, Ithaca, NY, 2005.
- [5] H. Padamsee, et al., RF Superconductivity for Accelerators, 1998.
- [6] P. Kneisel, in: Proceedings of the 2005 Workshop on RF Superconductivity, Ithaca, NY, 2005.
- [7] V. Shemelin, et al., in: Proceedings of the 2005 Particle Accelerator Conference, Knoxville, TN, 2005.
- [8] M.K. Kelly, et al., in: Proceedings of the 2003 Particle Accelerator Conference, Portland, OR, 2003.
- [9] R. Carcagno, et al., in: Proceedings of the 2003 Workshop on RF Superconductivity, Trarivue, 2003.
- [10] T. Grimm, et al., in: Proceedings of the 2004 LINAC, Luebeck, 2004.
- [11] P. Sekalski, et al., in: Proceedings of the 2005 Workshop on RF Superconductivity, Ithaca, NY, 2005.
- [12] M. Liepe, et al., in: Proceedings of the 2003 Particle Accelerator Conference, Portland, OR, 2003.
- [13] M. Liepe, et al., in: Proceedings of the 2005 Particle Accelerator Conference, Knoxville, TN, 2005.
- [14] B. Petersen, in: Proceedings of the 2005 Workshop on Energy-Recovery Linacs, Newport News, VA, 2005.